ACS APPLIED MATERIALS & INTERFACES

Research Article

Cite This: ACS Appl. Mater. Interfaces 2018, 10, 25819−25829

www.acsami.org

Superhydrophobic Photosensitizers: Airborne $^1O_2$ Killing of an in Vitro Oral Biofilm at the Plastron Interface

Smruti Pushalkar,[†] Goutam Ghosh,[‡] QianFeng Xu,[⊥] Yang Liu,[§,∥] Ashwini A. Ghogare,[‡,∥] Cecilia Atem,[†] Alexander Greer,*[,‡,∥,⊥] Deepak Saxena,*[,†] and Alan M. Lyons*[,§,∥,⊥]

[†]Department of Basic Sciences and Craniofacial Biology, New York University College of Dentistry, New York 10010, United States

[‡]Department of Chemistry, Brooklyn College, City University of New York, Brooklyn, New York 11210, United States

[§]Department of Chemistry, College of Staten Island, City University of New York, Staten Island, New York 10314, United States

[∥]Ph.D. Program in Chemistry, The Graduate Center of the City University of New York, 365 Fifth Avenue, New York, New York 10016, United States

[⊥]SingletO_2 Therapeutics LLC, 215 W 125th Street, 4th Floor, New York, New York 10027, United States

Supporting Information

ABSTRACT: Singlet oxygen is a potent agent for the selective killing of a wide range of harmful cells; however, current delivery methods pose significant obstacles to its widespread use as a treatment agent. Limitations include the need for photosensitizer proximity to tissue because of the short (3.5 μs) lifetime of singlet oxygen in contact with water; the strong optical absorption of the photosensitizer, which limits the penetration depth; and hypoxic environments that restrict the concentration of available oxygen. In this article, we describe a novel superhydrophobic singlet oxygen delivery device for the selective inactivation of bacterial biofilms. The device addresses the current limitations by: immobilizing photosensitizer molecules onto inert silica particles; embedding the photosensitizer-containing particles into the plastron (i.e. the fluid-free space within a superhydrophobic surface between the solid substrate and fluid layer); distributing the particles along an optically transparent substrate such that they can be uniformly illuminated; enabling the penetration of oxygen via the contiguous vapor space defined by the plastron; and stabilizing the superhydrophobic state while avoiding the direct contact of the sensitizer to biomaterials. In this way, singlet oxygen generated on the sensitizer-containing particles can diffuse across the plastron and kill bacteria even deep within the hypoxic periodontal pockets. For the first time, we demonstrate complete biofilm inactivation (>5 log killing) of *Porphyromonas gingivalis*, a bacterium implicated in periodontal disease using the superhydrophobic singlet oxygen delivery device. The biofilms were cultured on hydroxyapatite disks and exposed to active and control surfaces to assess the killing efficiency as monitored by colony counting and confocal microscopy. Two sensitizer particle types, a silicon phthalocyanine sol−gel and a chlorin e6 derivative covalently bound to fluorinated silica, were evaluated; the biofilm killing efficiency was found to correlate with the amount of singlet oxygen detected in separate trapping studies. Finally, we discuss the applications of such devices in the treatment of periodontitis.

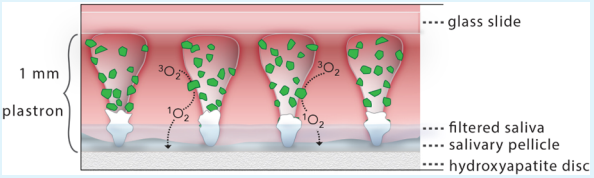

KEYWORDS: *superhydrophobic device, singlet oxygen, biofilm eradication, photodynamic therapy, dentistry*

1. INTRODUCTION

Bacterial inactivation methods commonly suffer from the potential for bacteria to develop resistance to the treatment. For example, antibiotics have been shown to kill bacteria without damaging the tissue, but can lose their effectiveness over time. Peroxides and other chemical oxidizing agents are less likely to lose their effectiveness, but these aggressive chemicals can lead to tissue inflammation and damage. Instead of a traditional chemical disinfectant, singlet oxygen [excited singlet delta ($^1\Delta_g$) $^1O_2$] has shown great promise in disinfection, in which it possesses a short lifetime prior to decaying back to ground-state oxygen.[1−5] Delivering singlet oxygen to the point of interest, and the preferential production of singlet oxygen over the other types of ROS, remains a barrier to effective treatment methods.[6]

Challenges to developing a singlet oxygen delivery system include the short lifetime of $^1O_2$; the low concentration of $^3O_2$ in hypoxic environments; the intense optical absorption of the sensitizer at the excitation wavelength; and the potential of the sensitizer molecules to stain or exhibit toxicity to tissues. These challenges are especially acute for periodontal pockets that can reach a depth of 10 mm. The lifetime of $^1O_2$ is only 3.5 μs in aqueous solutions, but ∼1 ms in air.[7] Thus, the transport length of $^1O_2$ is limited to ∼150 nm in aqueous liquids.[8] The partial pressure of $^3O_2$ source gas is less than 1300 Pa in human periodontal pockets,[9] which would reduce the rates of $^1O_2$ production without supplemental oxygen. Because

Received: June 6, 2018
Accepted: July 4, 2018
Published: July 4, 2018

DOI: 10.1021/acsami.8b09439
ACS Appl. Mater. Interfaces 2018, 10, 25819−25829

sensitizer molecules strongly absorb the excitation radiation (ε = ~0.003−0.20 cm^{-1} μM^{-1}), the quantity of light reaching the deeper periodontal pockets is reduced. This in turn reduces the concentration of singlet oxygen generated in deep pockets. Although some sensitizers are safe to use, such as Photofrin and rose bengal,[10] others have not been evaluated for toxicity. Even sensitizers that have been approved for direct contact with humans can cause unintended problems;[11] some compounds can leave a patient photosensitive to sunlight. Because of its safety, methylene blue has been introduced directly into the periodontal pocket to generate singlet oxygen in situ with an external light source; however, this method results in staining.[12,13] New sensitizers have been reported that color match with tooth enamel to avoid staining, but their toxicology is not yet known.[14] The isolation of the sensitizer from direct contact with biofluids and tissue would avoid the issues of staining and potential toxicity and so would be advantageous. Thus, a new technique for generating $^1O_2$ proximate to biofilms situated deep (3−10 mm) within the hypoxic pockets could be beneficial for bacterial inactivation and warrants further study.

Previous papers have reported on the external delivery of singlet oxygen. For example,[7] singlet oxygen bubbles were used to inactivate *Escherichia coli* and *Aspergillus fumigatus*, in which singlet oxygen diffused from the gas bubble into an aqueous solution to react with the target organism. This system delivered $^1O_2$ to the air/water interface of a solution, in which the sensitizer was isolated from the solution behind an ultrahigh-molecular-weight polyethylene membrane.[8] Using a different approach, a superhydrophobic (SH) surface was used to isolate the sensitizer from a solution containing a dissolved trapping agent.[15,16] The sensitizer remained dry, whereas singlet oxygen was generated on the sensitizer particles embedded in the plastron (i.e., the air layer beneath the water). Singlet oxygen was transported across the plastron and trapped in the solution. This approach demonstrates the utility of SH surfaces and the ability to transport $^1O_2$ to short distances (~1 mm) while retaining the ability to photo-oxidize organics in solution. Other airborne $^1O_2$ reactions have been useful for the reactions at solid surfaces, including the single-molecule detection of $^1O_2$ at a TiO_2 surface,[17−19] with $^1O_2$ in thin films[20] and in conjugated polymers,[21,22] and in $^1O_2$ bubbling systems in mass spectrometry.[23,24]

For dental applications, especially those associated with periodontal disease, it is necessary to kill the microorganisms within the biofilms attached to the cementum deep within the hypoxic pockets. The inactivation of biofilms is especially challenging as the bacteria within the biofilms can be significantly more resistant to oxidizing agents than the unattached cells.[25] As a result, a device is needed that can generate singlet oxygen proximate to the biofilm, while precluding sensitizer−tissue contact and while insuring adequate light fluence and oxygen concentration. Such a device could be used in a dental office to treat a patient's incipient infection or for prophylactic cleaning.

In this paper, we provide the first evidence for singlet oxygen inactivation of a periodontal biofilm via $^1O_2$ delivered from a solid sensitizer surface through the gas phase, as shown schematically in Figure 1. The SH surface is used to both prevent the contact between the sensitizer and the biofilm and insure a constant supply of $^3O_2$. Two types of photosensitizer particles were studied: a silicon phthalocyanine (Si-Pc) sol−gel and a chlorin e6 derivative covalently bound to fluorinated silica. The $^1O_2$ yield from these two particles was quantified in solution by trapping with a dissolved anthracene dipropionate dianion as well as the singlet oxygen-specific *trans*-2-methyl-2-pentenoate anion trap. The potential for photobleaching was measured by irradiating the particles before the singlet oxygen trapping experiments. For devices fabricated with both types of sensitizers, the tips of the surfaces were capped with inert silica nanoparticles to enhance the stability of the Cassie state, ensure the availability of $^3O_2$ across the entire surface, and preclude the direct contact of the sensitizer with the target *Porphyromonas gingivalis* biofilms. These biofilms were cultured on the disks of hydroxyapatite (HA), the primary mineral found in teeth. The light fluence threshold dose required for complete biofilm inactivation was determined by colony-forming units (CFU) counting and LIVE/DEAD staining with confocal imaging. Our results indicate that the SH sensitizer surface is capable of delivering $^1O_2$ and killing bacteria *without* the sensitizer coming in direct contact with the biofilm. Finally, an assessment of implementing the SH surface delivery technique for dental applications is presented.

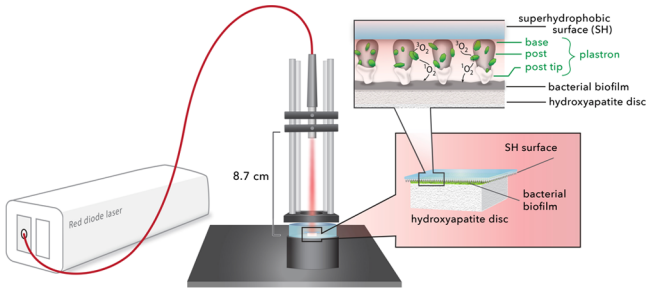

Figure 1. Schematic of the SH device: a red diode laser (669 nm) is coupled to an optical fiber; the output SMA ferrule is mounted such that the light is directed downward. The tip of the SH surface, printed on a 130 μm thick cover slip, is placed face-down on the bacterial biofilm. SiO_2 nanoparticles are used to cap the SH surface. Singlet oxygen traverses the plastron to reach the biofilm, where inactivation then takes place.

2. EXPERIMENTAL SECTION

2.1. Materials and Instrumentation. Silicon phthalocyanine dichloride ($SiPcCl_2$), chlorin e_6, 3-aminopropyltriethoxysilane (APTS), 3-glycidyloxypropyl-trimethoxysilane (GPTMS), 3-iodopropyl-trimethoxysilane, 3,3,4,4,5,5,6,6,6-nonafluorohexyltrimethoxysilane, hydrofluoric acid (HF), *trans*-2-methyl-2-pentenoate anion, 9,10-dibromo anthracene, *t*-butyl acrylate, *o*-tolylphosphine, potassium formate, palladium II acetate, triethylamine, trifluoroacetic acid, dimethylformamide, sodium hydroxide, toluene, acetonitrile, dichloromethane, and deuterium oxide-d_2 were purchased from Sigma-Aldrich (Allentown, PA). 9,10-Anthracene dipropionate dianion was synthesized in three steps and 76% yield using the procedure reported by Matsuo et al.[26] Porous Vycor glass (PVG) (Corning 7930) was purchased from Advanced Glass and Ceramics (Holden, MA) and ground to particles sized 40−150 μm in diameter. Silicone 3140 manufactured by Dow Corning (3140) was purchased from Ellsworth Adhesives (Germantown, WI). SiO_2 nanoparticles TS530 were obtained from the Cabot Corporation (Billerica, MA). The materials listed above were used as received without any further purification. The UV−vis spectra were collected with Hitachi U-2001 or Shimadzu-1800 spectrophotometers. The irradiance was measured using a visible-light-enhanced silicon photodetector (Newport Corp., Irvine, CA), which was calibrated for 400−1100 nm optical power measurements, and its maximum measurable power is 2.0 W. The temperature of the particles on the SH surface (SHS) was determined

DOI: 10.1021/acsami.8b09439
ACS Appl. Mater. Interfaces 2018, 10, 25819−25829

using a Testo 845 infrared temperature instrument (Lenzkirch, Germany) positioned above the surface.

2.2. Synthesis of Particles Si-Pc and e6 (Figure 2). *2.2.1. Particle Si-Pc.* The Si-Pc sol−gel particles were prepared using a literature source.[7,8,27] Briefly, 38.0 mg of $SiPcCl_2$ (6.2×10^{-5} mol) was added to 5 g of APTS (0.02 mol) and heated with stirring for 50 h at 120 °C under a nitrogen atmosphere. This yielded a bisamino Si-Pc derivative that was added to acidic ethanol and 23.6 g GPTMS (0.1 mol) and heated to 60 °C, before the temperature was lowered to 25 °C for 72 h. The Si-Pc sol−gel was filtered from ethanol, dried at 50 °C for 10 h, and then ground and sieved to particles sized 40−150 μm in diameter. Light green particles were obtained. The quantity of Pc present per gram of silica is 4.1 μmol Pc/g silica, which was measured from the weight of the sol−gel (15 g) and the amount of the Pc sensitizer (62 μmol) Figure 2.

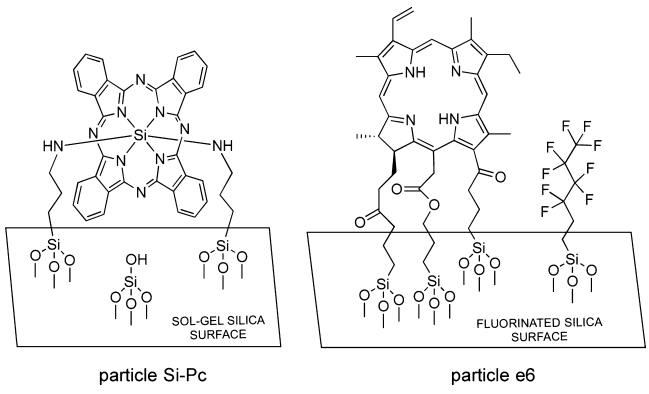

Figure 2. Two types of sensitizing particles examined (particles Si-Pc and e6). Particle Si-Pc has bisamino Si-phthalocyanine incorporated in a sol−gel. Particle e6 has chlorin covalently bound to fluorinated silica.

2.2.2. Particle e6. The chlorin-bound fluorinated silica particles were synthesized in three steps: (i) Fluorinated PVG particles (3.0 g) were added to 11.0 mmol of nonafluorohexyl-trimethoxysilane in 7 mL toluene and heated to reflux for 24 h for partially fluorinated silica and a coverage of 1.6 mmol nonafluorosilane/g PVG.[28] The particles were placed in a Soxhlet extractor with methanol for 24 h to remove any adsorbed fluorosilane. Approximately 1% of the SiOH groups were preserved for adhering of the sensitizer. (ii) Chlorin e_6 (40 mg, 0.068 mmol) was placed in 10 mL acetonitrile with triethylamine (90 μL, 0.64 mmol) and stirred for 15 min. Iodopropyl trimethoxysilane (60 μL, 0.3 mmol) was added in a dropwise fashion, and the mixture was refluxed for 48 h. Acetonitrile was then evaporated, leaving the chlorin trimethoxysilane conjugate. (iii) The chlorin trimethoxysilane conjugate was anchored to the remaining silanol sites of the fluorinated PVG particles (2.0 g) by adding them to the mixture and refluxing with toluene at 110 °C for 24 h. Dark green particles were obtained and washed with toluene, dichloromethane, and methanol, and then placed in a Soxhlet extractor with methanol for 24 h. As in the literature, the HF stripping treatment procedure[28] was used to determine the loading of the sensitizer onto fluorinated silica to be 1.4 μmol chlorin/g silica.

The images of the two particle types are shown in the Supporting Information, Figure S1.

2.3. SH Surfaces Fabricated with Si-Pc or e6 Particles. The process for printing SH surface posts has been reported previously.[29−31] The surfaces were printed in 1 cm^2 square (20 × 20) arrays with a pitch of 500 μm. Figure S2 shows, schematically, the three-dimensional (3D) printing of posts with Si-Pc or e6 particles partially embedded on the SH surface. Briefly, the SH surface posts were printed as posts (1000 μm tall, 500 μm pitch) forming a primary roughness. The sensitizer particles (Si-Pc or e6) were spread onto the posts immediately after printing and cured at 65 °C, creating a secondary roughness. The excess particles were removed by exposing the surface to the high flow of compressed air. The SH surface post-end tips were dipped into a thin layer of Corning 3140 silicone and coated with TS530-type SiO_2 nanoparticles. The tip-coated posts were cured at 65 °C in an oven with the tips facing down.

2.4. SH Surface for Bacterial Inactivation. Figure S3 shows the exposure apparatus with the sensitizer SH surface poised on the biofilm substrate. The light source was a CW diode laser (P_{max} = 0.7 W, 669 nm output, model 7404, Intense Ltd., North Brunswick, NJ). The laser optical energy was delivered through an FT-400-EMT optical fiber (numerical aperture 0.39; divergence angle 32°; 0.4 μm core diameter × 3 ft length) with an SMA 905 connector (Thorlabs, Inc., Newton, NJ) that produced a distribution of incident photons upon the top surface of a glass cover slip; the sensitizer-embedded SH surface was printed on the opposite surface. The distance between the fiber optic ferrule and the glass slide was 8.6 cm. A circular spot (diameter = 1 cm) was illuminated. The irradiance was measured with a visible-light silicon photodetector (Newport Corporation model #918D-SL-OD3R). This detector is calibrated for 400−1100 nm optical power measurements, and its maximum measurable power is 2.0 W. The amount of light dose (fluence) delivered to the surfaces was calculated by multiplying the irradiance by the exposure time. The experiments were carried out with static air, that is, gas was not sparged through the plastron. Because the cover slip and SH surface are lightweight, the polydimethylsiloxane (PDMS) posts do not become compressed, and so only the silica nanoparticle tips touch the biofilm.

2.5. Bacterial Culture. *P. gingivalis* ATCC 33277 was used in this study. The culture was grown on trypticase soy agar plates supplemented with 5% sheep blood with additional supplementation of menadione (0.3 μg/mL) and hemin (5 μg/mL). The culture was maintained anaerobically (80% N_2, 10% H_2, and 10% CO_2) at 37 °C.

2.6. Biofilm Preparation and Treatment. The biofilms were formed by inoculating log-phase grown *P. gingivalis* suspension (10^7 CFU/mL) to the wells of a sterile Petri dish (5 cm diameter) containing saliva-coated HA disks (0.38″ dia × 0.06″ thick, Clarkson Chromatography, PA, USA) in pre-reduced fastidious anaerobic broth (Lab M Limited, UK).

HA is an excellent synthetic substrate that mimics human dental tissues that can be coated with saliva for use as an oral biofilm model.[32,33]

The saliva-coated HA disks were prepared as described earlier.[34] The HA disks were incubated anaerobically at 37 °C for 72 h. The culture media were changed after 48 h. Following the biofilm formation at 72 h, the biofilms were washed three times in PBS. The disks were treated according to the treatment groups stated in the Results section. The *P. gingivalis* biofilms were treated with $^1O_2$ from the SH surfaces with and without sensitizers using various conditions in triplicate.

2.7. Detection of Viable Bacteria by CFUs. The biofilms from each of the treatment groups were tested for the total viable bacteria count. Initially, the disks were scraped to dislodge the bacteria attached to the surface and suspended in the pre-reduced media. Tenfold serial dilutions were performed and the samples were plated onto the blood agar plates and incubated anaerobically at 37 °C for 7 days. The viable counts of bacteria were calculated and interpreted in terms of log values of CFU per biofilm and as % killing. The reduction by ≥3 logs of the treated sample compared to the untreated control was considered bactericidal. All the experiments were performed in triplicates. The statistical analysis was carried out with the Student *t* test to determine the significance between individual treatments ($p < 0.05$ denoted significance).

2.8. Biofilm Analysis by Confocal Laser Scanning Microscopy. The bacterial biofilms were placed in six-well plates and stained using a LIVE/DEAD BacLight bacterial viability kit (Molecular Probes, Eugene, OR) with SYTO-9 (diluted to 5 mM) and propidium iodide (diluted to 30 mM). These biofilms had a thickness of approximately 63−81 μm and were incubated with the dyes in the dark at room temperature for 20−30 min before being imaged by a Zeiss LSM710 confocal-multiphoton microscope (Carl Zeiss Inc, NY, USA). All confocal laser scanning microscopy (CLSM) images were

DOI: 10.1021/acsami.8b09439
ACS Appl. Mater. Interfaces 2018, 10, 25819−25829

imaged within a window of 40−90 min after the application of the fluorescent dyes. At least five separate representative locations on the disks covered with biofilm were scanned, and the images were analyzed using ImageJ. Fluorescence intensity thresholds were set manually for each of the fluorescent colors. The 2D images were stacked for viewing as a 3D biofilm image. The CLSM software was set to take *z*-scans (*xyz*) of 1 μm thickness, and the image stacks were analyzed by Imaris software (Bitplane, USA).

2.9. Particle/Solution Dispersion System for the Detection of $^1O_2$ In Situ. Air-saturated solutions of either (a) 9,10-anthracene dipropionate dianion (**1**, 62 μM) in D_2O (1.0 mL) and 20 mg of sensitizer particles (Si-Pc or e6), or (b) *trans*-2-methyl-2-pentenoate anion (**3**, 62 mM) in D_2O (1.0 mL) as shown in Figure 3 and 100 mg

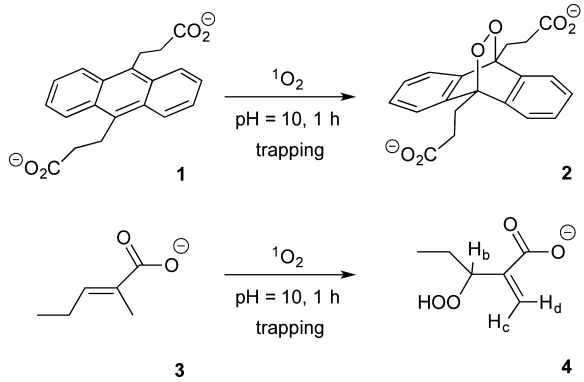

Figure 3. Photo-oxidation of the anthracene **1** and alkene **3** traps in a particle/solution dispersion via 669 nm irradiation of Si-Pc or e6 particles in D_2O. The particle surface is wetted and solution-phase $^1O_2$ is generated at the sensitizer particle surface. Evidence for a reaction of $^1O_2$ with **1** is the formation of endoperoxide **2** (quantified by the disappearance of a peak at 378 nm), and with **3** is the formation of hydroperoxide **4** (quantified by the appearance of the hydroperoxide peaks at H_b, H_c, and H_d by ^1H NMR).

of sensitizer particles (Si-Pc or e6) were irradiated with the 669 nm laser diode as shown in Figure S4. The pH of the solution was adjusted with NaOH to pH 10 to maintain the anionic forms of **1** and **3**. Some of the sensitizer particles sedimented to the bottom of the test tube because of their relatively high mass, and others remained dispersed in solution. The amount of singlet oxygen produced was estimated in situ by the reduction in the absorbance of the trapping agent **1** at 378 nm. The trapping agent forms endoperoxide **2** upon its reaction with singlet oxygen, and the endoperoxide does not absorb light at 378 nm. The amount of singlet oxygen produced was also estimated from the quantity of hydroperoxide **4** formed by monitoring the peaks in the nuclear magnetic resonance (NMR) spectrum of H_b, H_c, and H_d appearing at 4.75, 5.47, and 5.85 ppm, respectively.

3. RESULTS AND DISCUSSION

The efficacy of sensitizer particles containing Si-Pc or e6 molecules, for the generation of singlet oxygen and inactivation of *P. gingivalis* biofilms, was studied. In section 3.1, we describe a photochemical evaluation of the sensitizer particles for $^1O_2$ output and stability to photobleaching; in section 3.2, the fabrication of SH surfaces containing sensitizer particles partially embedded into them is described; in section 3.3, the inactivation of *P. gingivalis* biofilms with the SH photosensitizer surfaces; and in section 3.4, the aspects of the SH photosensitizer technique are described.

3.1. Sensitizer Particle Activity in Solution. To determine the relative performance of sensitizer particles, $^1O_2$ production was quantified by chemical trapping with 9,10-anthracene dipropionate dianion (**1**) and *trans*-2-methyl-2-pentenoate anion (**3**) in solution. Unlike 1,4-substituted naphthalenes,[35−37] 9,10-substituted anthracenes such as **1** are good $^1O_2$ trapping agents because they form the stable endoperoxide (**2**) with $^1O_2$, a reaction that is not readily reversible.[38−41] Figure 4 shows the results from Si-Pc and e6

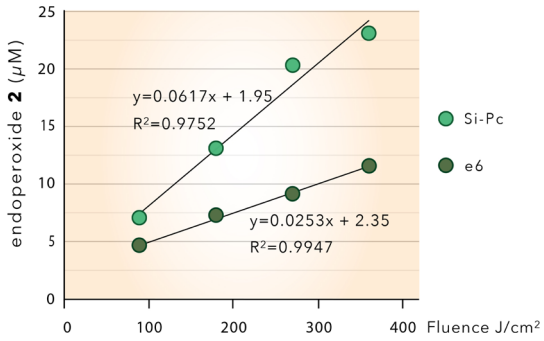

Figure 4. Singlet oxygen production by Si-Pc and e6 particles (20 mg) in D_2O solution (presaturated with O_2) plotted as a function of fluence. The singlet oxygen concentrations were estimated from the photo-oxidation of anthracene **1**. The Si-Pc or e6 particles were irradiated for 6, 12, 18, and 24 min at a constant irradiance of 0.25 W/cm^2.

particles (20 mg) dispersed in 1 mL of D_2O and illuminated with 669 nm light. The quantity of $^1O_2$ generated was estimated by the decrease in the absorption band of 9,10-anthracene dipropionate dianion **1** at 378 nm. D_2O was selected in favor of H_2O because of the 20-fold longer lifetime of $^1O_2$ in the deuterated solvent (65 μs compared to 3.5 μs),[42−44] as longer reaction times enhanced the yield and thus improved the resolution in the spectrophotometer.

The results show that on a per gram basis, the Si-Pc particles generate 2.4-fold higher quantities of $^1O_2$ than the e6 particles at any given fluence based on the linear regression lines for both, as in Figure 4. The increased effectiveness of the Si-Pc particles compared to the e6 particles may be explained, primarily, by the relative concentrations of the active sensitizer molecules bound to the particles. The concentration of sensitizer molecules in/on glass particles is 2.9-fold greater for the Si-Pc particles (4.1 μmol Si-Pc/g) compared to that for the e6 particles (1.4 μmol e6/g), as shown in the Supporting Information, Table S1. However, on a molar basis, the e6 sensitizer molecules produce singlet oxygen with more efficiency than Si-Pc (0.30 vs 0.24 nmol $^1O_2$ produced per nmol of the sensitizer, Table S1). This relatively higher molar efficiency of e6, compared to Si-Pc, is consistent with the relative efficiencies of chlorin versus phthalocyanine sensitizers for the singlet oxygen production reported in the literature.[45−56] The determination of the absolute efficiencies of the two sensitizer particles used in this study is complicated by several other factors, including surface coverage (the lower concentration of e6 per gram of particle is due, in part, to the nonafluorosilane coverage of 1.6 mmol/g silica, which preserved less than 1% of the SiOH groups for the binding of the e6 sensitizer); availability of the sensitizer molecules embedded within porous glass; and the determination of quantum yields and absorption coefficients of the sensitizer molecules chemically bonded to the surfaces. (See the Supporting Information Figure S5 and Table S1 for the absorption spectra and absorption coefficients, measured at 669 nm, of the two photosensitizers in solution.)

DOI: 10.1021/acsami.8b09439
ACS Appl. Mater. Interfaces 2018, 10, 25819−25829

A further indirect analysis of $^1O_2$ generation was carried out with the photo-oxidation of *trans*-2-methyl-2-pentenoate anion **3**, which formed the α,β-unsaturated hydroperoxide **4**. The "ene" reaction leads to the formation of hydroperoxide **4** bearing a shift of the double bond relative to **3**, which is a fingerprint for the presence of singlet oxygen.[57,58] In addition to **4**, only one other product was detected by NMR, a secondary alcohol corresponding to the deoxygenated hydroperoxide **4**. This degradation product of **4** was observed, as expected. There were no by-products associated with the oxidation of **3** that could be formed by the other types of radical-like reactive oxygen species.

Furthermore, the results of trapping with **3** show that the Si-Pc particles generate 2.3-fold higher quantities of $^1O_2$ than the e6 particles, which are very similar to the results of trapping with **1** that show that the Si-Pc particles generate 2.4-fold higher quantities of $^1O_2$ than the e6 particles. Because the oxidation of **3** to **4** is selective for singlet oxygen, we conclude that singlet oxygen is the key oxidant in both trapping reactions.

Photobleaching of sensitizers can degrade singlet oxygen generation[59−62] and has the potential to affect our results. The effect of irradiating particles at 669 nm in air prior to trapping measurements was studied using both types of particles dispersed in solution. Figure 5 shows the trapping by **1** of $^1O_2$ generated from the pristine Si-Pc and e6 particles in D_2O at 0.25 W/cm^2 for 15 min (left-hand columns). When the particles were pre-irradiated at 0.25 W/cm^2 for 45 min in air and then examined for $^1O_2$ production in D_2O, the results were found to be the same within experimental error (Figure 5, right-hand columns) as the pristine particles. These results demonstrate that the photobleaching of the particles does not occur under the experimental conditions used in this study.

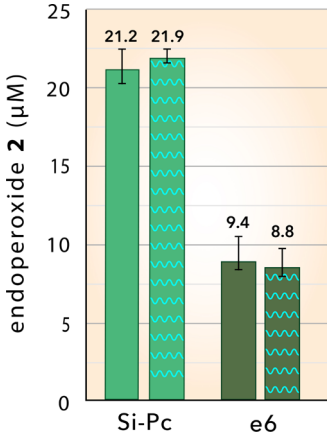

Figure 5. Photobleaching evaluation: singlet oxygen production based on the formation of endoperoxide **2** by the oxidation of anthracene **1** by Si-Pc and e6 particles dispersed in D_2O solution at 0.25 W/cm^2 for 15 min (fluence = 270 J/cm^2). The left-hand (solid) columns indicate the values using particles without preirradiation, whereas the right-hand columns (cross-hatched) were from the particles pre-irradiated at 0.25 W/cm^2 for 45 min in air (fluence = 675 J/cm^2), prior to the singlet oxygen trapping measurement.

3.2. Fabrication of SH Sensitizer Surfaces. The surfaces containing arrays of PDMS posts on glass cover slip substrates were fabricated using a modified 3D printing technique. The conical posts have a circular base (~500 μm diameter) and a height of 1000 μm on a 500 μm pitch. The 20 × 20 square arrays cover an area of 1 cm^2. The surfaces were prepared with both types of sensitizer particles and capped with hydrophobic silica nanoparticles. The surfaces without sensitizer particles were prepared as controls.

The silica−PDMS caps serve two purposes: they increase the stability of the SH (i.e., Cassie) state and prevent the direct contact of the sensitizer particles with the biofilm. The silica nanoparticles used for the cap are small, with a primary particle size of <20 nm, resulting in a high surface area (225 m^2/g). In addition, the nanoparticles are coated with hexamethyldisilazane, resulting in a low surface energy, similar to the surface energy of the underlying PDMS. This combination of high surface area and low surface energy results in stable SH properties. Thus, transitions from the SH Cassie state to the wetted Wenzel state, which could cause the liquids to wet into the plastron and thus contact the sensitizer particles, are unlikely at pressures below 500 kPa.[30] Figure 6 illustrates the enhanced Cassie-state stability of the capped sensitizer surfaces. A droplet of water poised on a chlorin e6 SH surface assumes the Cassie state as shown in Figure 6a. A higher magnification view (Figure 6b) shows the partial wetting of the hydrophobic chlorin e6 particles. The increased surface area and hydrophobicity of the nanoparticle silica-capped Si-Pc SH surface, shown in Figure 6c, result in less infiltration of water into the plastron.

Figure S6a in the Supporting Information is an optical micrograph of an SH surface with Si-Pc particles partially embedded into the surface immersed in a Petri dish of water, demonstrating how effectively the SH surface excludes liquid water from the plastron. Figure S6b illustrates an individual water droplet poised on the SH surface.

3.3. Bacterial Inactivation. *3.3.1. Effect of Fluence on Biofilm Inactivation Using Si-Pc SHS.* The antimicrobial effect of SH surfaces with Si-Pc particles (Si-Pc SHS) was evaluated in a light dose-dependent manner on *P. gingivalis* biofilms grown on HA disks. An SH surface with no sensitizer particles exposed to light (SH+ L+ S−) was used as an internal control. The biofilm itself, without an SH surface and no exposure to light (SH− L− S−), was used as an experimental control; the inactivation efficiency of the SH surfaces was quantified relative to this control for all our experiments. The biofilm inactivation was studied by treating the bacterial biofilms with the Si-Pc SHS at irradiance values of 0.1, 0.2, 0.3, or 0.35 W/cm^2 for either 7.5 or 15 min, yielding a series of fluence values of 45, 90, 180, 270, and 315 J/cm^2 (SH+ L+ S+).

The results, shown in Figure 7a, indicate a clear threshold for the inactivation of *P. gingivalis* biofilms. The bactericidal effect on the biofilms was significant ($p \leq 0.05$) when treated with Si-Pc SHS at a fluence of 270 J/cm^2 or higher. At this fluence, a marked 6 log reduction in bacterial viability was observed compared to controls. At a higher fluence of 315 J/cm^2, the killing efficiency was increased to greater than 6 log reduction with no viable cells observed (bar too small to appear in Figure 7a). In contrast, the viability of bacteria, as measured by the log of CFUs/biofilm, was not significantly altered in the presence of the control surfaces exposed to light, but without sensitizer particles (SH+ L+ S−), over the range of fluence values from 45 to 180 J/cm^2. The biofilms exposed to SH+ L+ S− controls at higher fluence values (270 and 315 J/cm^2) showed the bacterial viability lowered by 1 log, but this reduction was not statistically significant. This suggests that the SH surfaces were bactericidal in the presence of the sensitizer

DOI: 10.1021/acsami.8b09439
ACS Appl. Mater. Interfaces 2018, 10, 25819−25829

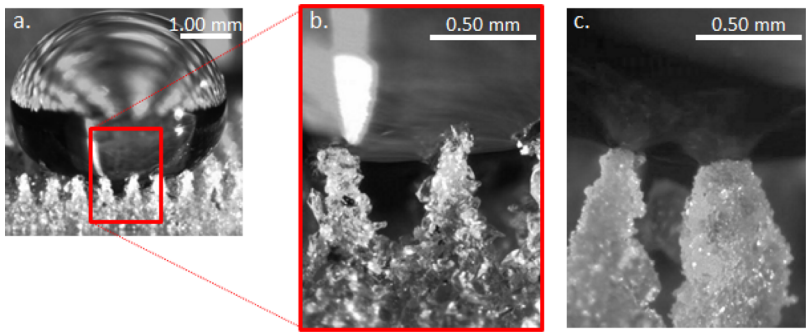

Figure 6. Water droplet poised on SH surfaces. (a) Low-magnification view of water on an SH surface with chlorin e6 particles without PDMS−silica caps. (b) High-magnification view showing the water partially wetting the upper e6 particles. (c) High-magnification view of a Si-Pc SH surface capped with PDMS−silica nanoparticles; water penetration is limited because of the high surface area and low surface energy nanoparticle coating.

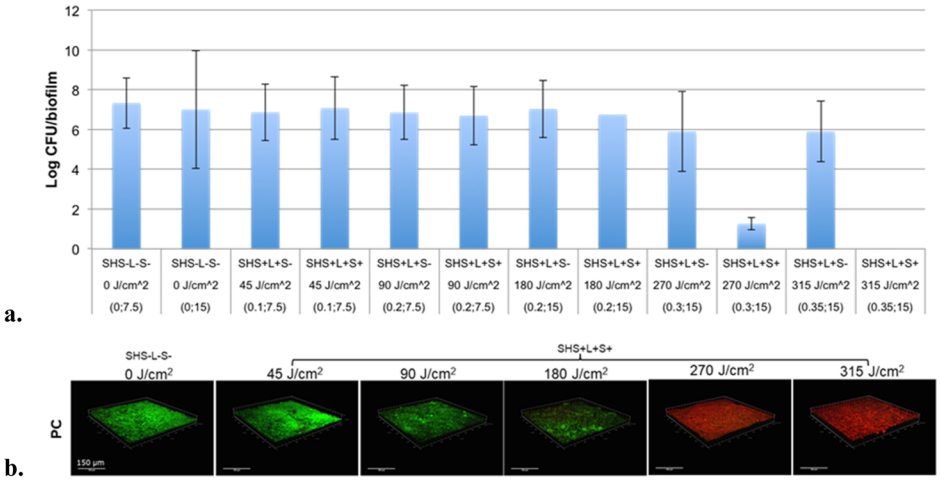

Figure 7. (a) *P. gingivalis* inactivation by SH surfaces as a function of fluence (J/cm^2), measured by CFUs after exposure. The biofilm-only controls without light (SH− L− S−) were incubated for 7.5 and 15 min, respectively. The sensitizer-less SH surfaces (SH+ L+ S−) and SH surfaces with Si-Pc (SH+ L+ S+) were exposed to the fluence values of 45, 90, 180, 270, and 315 J/cm^2. The data are expressed as mean ± SEM of three independent experiments, $n = 3$. *$p < 0.05$. The numbers in the parentheses refer to the irradiance values of 0, 0.1, 0.2, 0.3, or 0.35 W/cm^2 at either 7.5 or 15 min. (b) Representative 3D images of 72 h grown *P. gingivalis* biofilms following treatment with a Si-Pc SH surface. The photoinactivation effect on the biofilms as rendered by Si-Pc SHS at variable light doses, compared to biofilm-only control without light treatment. Green signal represents viable cells (Syto 9); red signal indicates damaged/dead cells (propidium iodide). The panels are of *xyz*-stacks of biofilm growth.

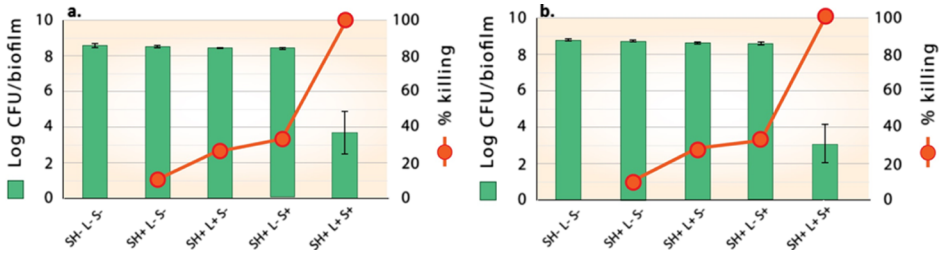

Figure 8. Inactivation of *P. gingivalis* biofilms by Si-Pc SH surfaces and controls at fluences of (a) 270 J/cm^2 (*$p < 0.006$) and (b) 315 J/cm^2 (*$p < 0.003$). The inactivation of bacterial biofilms is shown as a log viable count and percentage killing. The data are expressed as mean ± SEM of three independent experiments, $n = 3$.

Si-Pc and red light. Li et al.[63] showed 3 log and 5 log reduction with cationic zinc phthalocyanines on *E. coli* biofilms by photodynamic antimicrobial chemotherapy.

To reaffirm the CFU count results, the viability or inactivation of 72 h grown *P. gingivalis* biofilms on the saliva-coated HA disks was assessed by CLSM based on the detection of green (live bacteria) and red (dead bacteria) fluorescence. Figure 7b represents a subset of 3D bacterial biofilms at different light fluence values, 45, 90, 180, 270, and 315 J/cm^2, in the presence of Si-Pc SH surfaces (SH+ L+ S+), compared to the biofilm-only control (SH− L− S−). The results indicate that the viability of the biofilms was not compromised significantly until a fluence of 180 J/cm^2 was reached. A maximum bactericidal activity was observed with the Si-Pc SHS at the fluence doses of 270 and 315 J/cm^2 (Figure 7b). Thus, the CLSM imaging results confirm the CFU count results and establish a threshold fluence of 270 J/cm^2.

DOI: 10.1021/acsami.8b09439
ACS Appl. Mater. Interfaces 2018, 10, 25819−25829

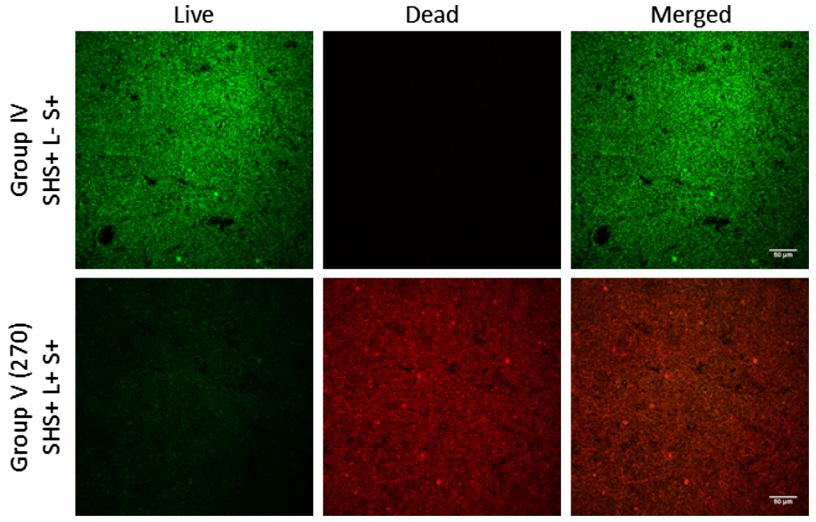

Figure 9. Representative images of *P. gingivalis* biofilms following each treatment group with Si-Pc SHS and controls. Green signal represents viable live cell (Syto 9); red signal indicates damaged/dead cells (propidium iodide). Image panels: live, dead, and merged (live + dead) are the $x-y$ plane images.

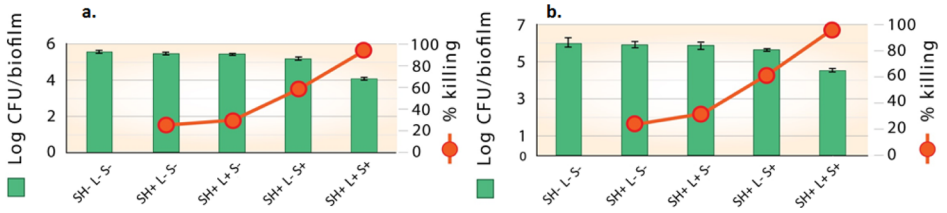

Figure 10. Inactivation of *P. gingivalis* biofilms by e6 SH surfaces and controls at fluences of (a) 270 J/cm^2 (*p < 0.0002) and (b) 315 J/cm^2 (*p < 0.006). The inactivation of bacterial biofilms is shown as log viable count and percentage killing. The data are expressed as mean ± SEM of three independent experiments, n = 3.

With the fluence thresholds established, we conducted our next experiments with the fluence values of 270 and 315 J/cm^2 to compare the bacterial inactivation efficiency of the sensitizer particles, Si-Pc and e6.

3.3.2. Effect of Sensitizer Particle Type on Biocidal Efficiency of SH Surfaces. To quantify the effect of particle type, the inactivation of *P. gingivalis* biofilms with Si-Pc and e6 SH surfaces was studied using an expanded group of controls; the results are shown in Figures 8−10. The SH surfaces with sensitizer particles (SH+ L+ S+) were placed onto the HA disks with bacterial biofilms and were irradiated using a fluence of 270 or 315 J/cm^2 (irradiance of 0.30 or 0.35 W/cm^2 for 15 min, respectively). In addition, four types of controls were included in these trials. The experimental control was the biofilm itself without any exposure to an SH surface (SH− L− S−). To determine how the PDMS SH surface without sensitizer particles affected the biofilm, two internal controls were included with and without exposure to light (SH+ L+ S− and SH+ L− S−). The fourth test control was composed of SH surfaces with particles (Si-Pc or e6), but without exposure to light (SH+ L− S+), which were used to determine the effect of SH-embedded sensitizers on bacteria in the absence of photoactivation. Table S2 in the Supporting Information summarizes the control and experimental samples.

The SH surfaces containing sensitizer particles attained maximum bactericidal effects in the presence of light (Figures 8−10), which indicates the high singlet oxygen production at these fluence values. All four controls exhibited low bacterial inactivation values.

3.3.2.1. Si-Pc SH Surfaces. For the Si-Pc SH surfaces, a marked bactericidal effect was observed with ≥5 log reduction and absolute killing of 99.99%, at irradiances of 270 J/cm^2 (Figure 8a) and 315 J/cm^2 (Figure 8b). These results support our hypothesis that singlet oxygen generated in the plastron of the SH surface reaches the bacteria at a sufficient concentration to achieve effective killing, as only those surfaces having sensitizer particles exposed to light exhibit significant reductions in viability (>4 log reduction in CFU). Light with sensitizer-less SH surface (SH+ L+ S−) showed substantially lower effectiveness (26−29% killing at 270 and 315 J/cm^2), as did the Si-Pc SHS in the absence of light (SH+ L− S+, ∼33% reduction). The control experiments with sensitizer-less SH surface without light (SH+ L− S−) showed only ∼10% killing at 270 and 315 J/cm^2.

To affirm the CFU count results, the viability of 72 h grown *P. gingivalis* biofilms on the saliva-coated HA disks was assessed by CLSM based on the detection of green (live bacteria) and red (dead bacteria) fluorescence. Figure 9 represents a subset of the CLSM results; a control Si-Pc SH surface without illumination (top row) is compared with the same Si-Pc SHS illuminated with a fluence of 270 J/cm^2 (bottom row). The control (SHS+ L− S+) contains numerous live bacteria (bright green) with essentially no evidence for the presence of dead bacteria. In contrast, essentially all bacteria in the treated biofilm (SHS+ L+ S+) appear dead (red). The CLSM results for all five controls, as well as the surfaces illuminated with the fluences of 270 and 315 J/cm^2, are shown in the Supporting

DOI: 10.1021/acsami.8b09439
ACS Appl. Mater. Interfaces 2018, 10, 25819−25829

Information, Figure S7. All the CLSM images confirm the CFU count results.

3.3.2.2. e6 SH Surfaces. The SH surfaces with e6 particles also attained a marked reduction in biofilm viability; however, the effect was smaller than that for Si-Pc particles. The e6 SH surfaces achieved ∼97% killing with an approximate 1.5 log reduction of CFU when exposed to the fluences of 270 J/cm^2 (Figure 10a) and 315 J/cm^2 (Figure 10b), as compared to their corresponding biofilm-only controls. The control experiments with sensitizer-less SH surface without light (SH+ L− S−) showed 24% killing at 270 and 315 J/cm^2. The addition of light to an SH surface without sensitizer particles (SH+ L+ S−) resulted in a small increase in the percentage of killing (approximately 31−33%) relative to the biofilm-only controls. The presence of e6 sensitizer, but without light (SH+ L− S+), displayed 59.13 and 60.84% microbicidal activity at 270 and 315 J/cm^2, respectively (Figures 10a and 10b). Similar to the Si-Pc SHS evaluations, the CLSM results confirmed the CFU count results as shown in the Supporting Information, Figure S8.

Both types of surfaces with sensitizer particles, Si-Pc and e6, in the presence of light, exhibited significant bactericidal effect on *P. gingivalis* biofilms ($p < 0.05$) (Figures 8−10). However, the Si-Pc SH surfaces are more effective than the surfaces prepared with an equal mass of e6 particles. This higher efficiency of the Si-Pc SH surfaces results from the larger number of sensitizer molecules per gram of particle, as discussed in section 3.1. No statistically significant differences were observed when comparing the biofilm inactivation efficiency between the biofilm-only controls and other internal controls.

3.4. Critical Aspects of the SH Surface Results. *3.4.1. Advantages of an SH System.* Plastron-derived $^1O_2$ provides a unique treatment approach to biofilm inactivation, as shown schematically in Figure 1 and in more detail in the Supporting Information, Figure S9. The sensitizer in the particle absorbs light and converts $^3O_2$ to its first singlet state (S_1) and then to the excited triplet state (T_1) via intersystem crossing. From T_1, the energy is transferred to $^3O_2$, generating airborne $^1O_2$, which travels a relatively short distance (<1 mm) below the biofilm. Singlet oxygen will oxidize the sites on the bacterium and kill the bacteria after a threshold dose is reached.

The SH surface is coated with sensitizer particles except at the tips, which are capped with a layer of SiO_2 nanoparticles. This hierarchical structure of the particle-embedded SH surface ensures that the region between PDMS posts (i.e., plastron) is a continuous space that remains filled with air, as the biofilm and associated fluids cannot penetrate this SH barrier. As a result, a supply of $^3O_2$ is readily available to all sensitizer particle surfaces. Diffusion of $^3O_2$ through a biofluid to reach the sensitizer is not necessary. Thus, the overall efficiency of $^1O_2$ generation is expected to be relatively higher compared to the systems where oxygen diffusion through a biofluid or biofilm into a hypoxic pocket is required. Moreover, the entire surface remains fully exposed to the excitation illumination; particle absorption does not affect the penetration depth.

It is noted that $^1O_2$ is highly sensitive to the environment, and the $^1O_2$ lifetime can be quenched through collisions with active species. For example, the lifetime of $^1O_2$ in air (∼1 ms) is long compared to its lifetime in water (3.5 μs). This sensitivity to environment can be exploited as $^1O_2$ is formed in the plastron, which is a dry environment where the diffusion length is approximately 1 mm. In contrast, $^1O_2$ can only diffuse ∼100−200 nm in solution before quenching. The longer (∼1 mm) diffusion distance of airborne $^1O_2$ permits this reactive gas, generated in the plastron, to reach and kill the *P. gingivalis* biofilm resting on the tips of the SH surface. Moreover, sensitizers are resistant to bleaching processes when present in air, as compared to the liquid environments. Thus, photobleaching was not observed in our experiments.

The silica-capped SH surface provides an additional advantage because the biofilm avoids direct contact with the sensitizer, and the potential for staining, inflammation, and toxicity is minimized. Ideally, the use of FDA-approved sensitizer molecules would be preferable. In this way, an inadvertent loss of adhesion at the sensitizer−PDMS interface would pose no chance for harm.

3.4.2. Particle Type and Threshold Dose. We have demonstrated that sensitizer loading in/on the glass particles determines the fluence required for biofilm inactivation. The amount of Si-Pc sensitizer in the sol−gel was 4.1 μmol Pc/g sol−gel, and the amount of chlorin e_6 was 1.4 μmol/g fluorinated silica. The larger number of sensitizer molecules per gram accounts for greater effectiveness of Si-Pc particles when equal sensitizer particle weights are used. The higher absorption of Si-Pc at 669 nm also contributes to this greater activity. Neither SH surface (Si-Pc or e6) photobleaches after 0.25 W/cm^2 for 45 min (fluence = 675 J/cm^2) because the percent yield of the endoperoxide **2** and hydroperoxide **4** was the same regardless of whether the particles were pre-irradiated or not (Figure 5). We also know the fluence threshold required to achieve a 5 log reduction of CFUs (∼300 J/cm^2) is higher than the thresholds reported in the literature[64] for the systems where particles are dispersed in solution and come into direct contact with the trapping agent. This higher threshold may result from the singlet oxygen decay that occurs as the reactive oxygen species traverse the distance between the sensitizer surface, where they are generated, and the live biofilm.

3.4.3. Dental Application. The amount of time required for complete biofilm deactivation, less than 15 min, is consistent with an in-office dental treatment therapy. Miniaturization of the device, so that it can be directly inserted into a periodontal pocket, is underway.

4. CONCLUSIONS

The inactivation of a bacterial biofilm using an SH photodynamic therapy technique that generates $^1O_2$ has been studied for the first time. The isolation of sensitizer molecules in the plastron of the device was shown to be both effective and advantageous; a constant supply of oxygen is maintained, whereas the direct contact of the sensitizer to biomaterials is avoided. An important point to highlight is that heterogeneous sensitizers are (in general) reported to have good photostability, even more so than the solvated sensitizers in solution.[65] Therefore, another virtue of the sensitizer being immobilized in an SH surface is its good photostability. Additionally, *P. gingivalis* is an anaerobic organism that is harmed by the presence of oxygen that can be exploited by using a stream of oxygen to kill the bacteria. That the periodontal pocket creates an anaerobic environment means, based on our previous work,[7,8] that singlet oxygen should be more effective when treating bacteria in the mouth.

Future work will focus on: (i) increasing the density of sensitizer triplet-excited states located within the SH surface

DOI: 10.1021/acsami.8b09439
ACS Appl. Mater. Interfaces 2018, 10, 25819−25829

plastron to further increase the $^1O_2$ output and reduce the treatment times; (ii) flowing $^3O_2$ gas across the SH surface to increase the mass transport of singlet oxygen from the plastron to the bacterium; (iii) evaluating the effectiveness of this technique with other bacteria and saliva biofilms; and (iv) fabricating a handheld PDT device[66] that incorporates an SH sensitizer surface, which can be directly inserted into a periodontal pocket. Such a device would be a useful tool for treating peri-implantitis and endodontic infections in a dental office.

■ ASSOCIATED CONTENT

Supporting Information

The Supporting Information is available free of charge on the ACS Publications website at DOI: 10.1021/acsami.8b09439.

Illustrations of the device, live/dead images of biofilms, optical images, and other information of the sensitizer particles (PDF)

■ AUTHOR INFORMATION

Corresponding Authors

*E-mail: agreer@brooklyn.cuny.edu (A.G.).
*E-mail: ds100@nyu.edu (D.S.).
*E-mail: Alan.Lyons@csi.cuny.edu (A.M.L.).

ORCID

Yang Liu: 0000-0003-4978-6051
Alexander Greer: 0000-0003-4444-9099
Deepak Saxena: 0000-0002-5506-5827

Notes

The authors declare the following competing financial interest(s): Alexander Greer is co-founder and CTO and Alan Lyons is co-founder and COO of SingletO2 Therapeutics LLC.

■ ACKNOWLEDGMENTS

The authors acknowledge the support from the National Institute of Dental and Craniofacial Research (NIH R41DE026083). A.G. acknowledges support from a Leonard and Claire Tow Professorship at Brooklyn College. The authors thank Leda Lee for the graphic arts work and Alison Domzalski for the photography work. They also thank Dr. Prabhu Mohapatra for synthesizing the 9,10-anthracene dipropionate dianion and Dr. Yan Deng from the NYULMC core microscopy facility for the CLSM image processing. A.G. wishes to dedicate this paper to William W. Greer (D.M.D.).

■ REFERENCES

(1) *Singlet Oxygen: Applications in Biosciences and Nanosciences*; Nonell, S., Flors, C., Eds.; Royal Society of Chemistry: Oxfordshire, U.K., 2016; pp 1−450.

(2) Pryor, W. A.; Houk, K. N.; Foote, C. S.; Fukuto, J. M.; Ignarro, L. J.; Squadrito, G. L.; Davies, K. J. A. Free Radical Biology and Medicine: It's a Gas, Man! *Am. J. Physiol.: Regul., Integr. Comp. Physiol.* **2006**, *291*, R491−R511.

(3) Krinsky, N. I. Biological Roles of Singlet Oxygen. In *Singlet Oxygen*; Wasserman, H. H., Ed.; Academic Press, 1979; Vol. *40*, pp 597−641.

(4) Maisch, T.; Baier, J.; Franz, B.; Maier, M.; Landthaler, M.; Szeimies, R.-M.; Baumler, W. The Role of Singlet Oxygen and Oxygen Concentration in Photodynamic Inactivation of Bacteria. *Proc. Natl. Acad. Sci. U.S.A.* **2007**, *104*, 7223−7228.

(5) Felgenträger, A.; Maisch, T.; Späth, A.; Schröder, J. A.; Bäumler, W. Singlet Oxygen Generation in Porphyrin-Doped Polymeric Surface Coating Enables Antimicrobial Effects on *Staphylococcus aureus*. *Phys. Chem. Chem. Phys.* **2014**, *16*, 20598−20607.

(6) Callaghan, S.; Senge, M. O. The Good, the Bad, and the Ugly—Controlling Singlet Oxygen Through Design of Photosensitizers and Delivery Systems for Photodynamic Therapy. *Photochem. Photobiol. Sci.* **2018**, in press. DOI: 10.1039/C8PP00008E

(7) Bartusik, D.; Aebisher, D.; Lyons, A. M.; Greer, A. Bacterial Inactivation by a Singlet Oxygen Bubbler: Identifying Factors Controlling the Toxicity of $^1O_2$ Bubbles. *Environ. Sci. Technol.* **2012**, *46*, 12098−12104.

(8) Bartusik, D.; Aebisher, D.; Ghafari, B.; Lyons, A. M.; Greer, A. Generating Singlet Oxygen Bubbles: A New Mechanism for Gas-Liquid Oxidations in Water. *Langmuir* **2012**, *28*, 3053−3060.

(9) Tanaka, M.; Hanioka, T.; Takaya, K.; Shizukuishi, S. Association of Oxygen Tension in Human Periodontal Pockets With Gingival Inflammation. *J. Periodontol.* **1998**, *69*, 1127−1130.

(10) Kessel, D.; Foster, T. H. Introduction to the Symposium-in-Print: Photodynamic Therapy. *Photochem. Photobiol.* **2007**, *83*, 995.

(11) Kim, M. M.; Ghogare, A. A.; Greer, A.; Zhu, T. C. On the in vivo photochemical rate parameters for PDT reactive oxygen species modeling. *Phys. Med. Biol.* **2017**, *62*, R1−R48.

(12) Theodoro, L. H.; Lopes, A. B.; Nuernberg, M. A. A.; Cláudio, M. M.; Miessi, D. M. J.; Alves, M. L. F.; Duque, C.; Mombelli, A.; Garcia, V. G. Comparison of repeated applications of aPDT with amoxicillin and metronidazole in the treatment of chronic periodontitis: A short-term study. *J. Photochem. Photobiol., B* **2017**, *174*, 364−369.

(13) Andersen, R.; Loebel, N.; Hammond, D.; Wilson, M. Treatment of Periodontal Disease by Photodisinfection Compared to Scaling and Root Planing. *Int. J. Clin. Dent.* **2007**, *18*, 34−38.

(14) Späth, A.; Leibl, C.; Cieplik, F.; Lehner, K.; Regensburger, J.; Hiller, K.-A.; Bäumler, W.; Schmalz, G.; Maisch, T. Improving Photodynamic Inactivation of Bacteria in Dentistry: Highly Effective and Fast Killing of Oral Key Pathogens with Novel Tooth-Colored Type-II Photosensitizers. *J. Med. Chem.* **2014**, *57*, 5157−5168.

(15) Aebisher, D.; Bartusik, D.; Liu, Y.; Zhao, Y.; Barahman, M.; Xu, Q.; Lyons, A. M.; Greer, A. Superhydrophobic Photosensitizers. Mechanistic Studies of $^1O_2$ Generation in the Plastron and Solid/Liquid Droplet Interface. *J. Am. Chem. Soc.* **2013**, *135*, 18990−18998.

(16) Zhao, Y.; Liu, Y.; Xu, Q.; Barahman, M.; Bartusik, D.; Greer, A.; Lyons, A. M. Singlet Oxygen Generation on Porous Superhydrophobic Surfaces: Effect of Gas Flow and Sensitizer Wetting on Trapping Efficiency. *J. Phys. Chem. A* **2014**, *118*, 10364−10371.

(17) Naito, K.; Tachikawa, T.; Cui, S.-C.; Sugimoto, A.; Fujitsuka, M.; Majima, T. Single-Molecule Detection of Airborne Singlet Oxygen. *J. Am. Chem. Soc.* **2006**, *128*, 16430−16431.

(18) Setsukinai, K.-i.; Urano, Y.; Kakinuma, K.; Majima, H. J.; Nagano, T. Development of Novel Fluorescence Probes That Can Reliably Detect Reactive Oxygen Species and Distinguish Specific Species. *J. Biol. Chem.* **2003**, *278*, 3170−3175.

(19) Naito, K.; Tachikawa, T.; Fujitsuka, M.; Majima, T. Real-Time Single-Molecule Imaging of the Spatial and Temporal Distribution of Reactive Oxygen Species with Fluorescent Probes: Applications to TiO_2 Photocatalysts. *J. Phys. Chem. C* **2008**, *112*, 1048−1059.

(20) Fudickar, W.; Fery, A.; Linker, T. Reversible Light and Air-Driven Lithography by Singlet Oxygen. *J. Am. Chem. Soc.* **2005**, *127*, 9386−9387.

(21) Altınok, E.; Smith, Z. C.; Thomas, S. W., III Two-Dimensional, Acene-Containing Conjugated Polymers That Show Ratiometric Fluorescent Response to Singlet Oxygen. *Macromolecules* **2015**, *48*, 6825−6831.

(22) Frausto, F.; Thomas, S. W., III Ratiometric Singlet Oxygen Detection in Water Using Acene-Doped Conjugated Polymer Nanoparticles. *ACS Appl. Mater. Interfaces* **2017**, *9*, 15768−15775.

(23) Lu, W.; Sun, Y.; Zhou, W.; Liu, J. pH-Dependent Singlet O_2 Oxidation Kinetics of Guanine and 9-Methylguanine: An Online Mass Spectrometry and Spectroscopy Study Combined with Theoretical Exploration. *J. Phys. Chem. B* **2018**, *122*, 40−53.

(24) Sun, Y.; Lu, W.; Liu, J. Exploration of the Singlet O_2 Oxidation of 8-Oxoguanine by Guided-Ion Beam Scattering and Density Functional Theory: Changes of Reaction Intermediates, Energetics, and Kinetics upon Protonation/Deprotonation and Hydration. *J. Phys. Chem. B* **2017**, *121*, 956−966.
(25) LeChevallier, M. W.; Cawthon, C. D.; Lee, R. G. Inactivation of Biofilm Bacteria. *Appl. Environ. Microbiol.* **1988**, *54*, 2492−2499.
(26) Matsuo, K.; Nakagawa, H.; Adachi, Y.; Kameda, E.; Aizawa, K.; Tsumoto, H.; Suzuki, T.; Miyata, N. Photoinduced Upregulation of Calcitonin Gene-Related Peptide in A549 Cells Through HNO Release from a Hydrophilic Photocontrollable HNO Donor. *Chem. Pharm. Bull.* **2012**, *60*, 1055−1062.
(27) Xia, H.; Nogami, M.; Hayakawa, T.; Imaizumi, D. Solid Type Silicon-Phthalocyanine-Conjugated Hybrids with Strong Optical Limiting Effect. *J. Mater. Sci. Lett.* **1999**, *18*, 1837−1839.
(28) Bartusik, D.; Aebisher, D.; Ghosh, G.; Minnis, M.; Greer, A. Fluorine End-Capped Optical Fibers for Photosensitizer Release and Singlet Oxygen Production. *J. Org. Chem.* **2012**, *77*, 4557−4565.
(29) Barahman, M.; Lyons, A. M. Ratchetlike Slip Angle Anisotropy on Printed Superhydrophobic Surfaces. *Langmuir* **2011**, *27*, 9902−9909.
(30) Xu, Q. F.; Mondal, B.; Lyons, A. M. Fabricating Superhydrophobic Polymer Surfaces with Excellent Abrasion Resistance by a Simple Lamination Templating Method. *ACS Appl. Mater. Interfaces* **2011**, *3*, 3508−3514.
(31) Xu, Q. F.; Liu, Y.; Lin, F.-J.; Mondal, B.; Lyons, A. M. Superhydrophobic TiO_2-Polymer Nanocomposite Surface with UV-Induced Reversible Wettability and Self-Cleaning Properties. *ACS Appl. Mater. Interfaces* **2013**, *5*, 8915−8924.
(32) Jaffar, N.; Miyazaki, T.; Maeda, T. Biofilm Formation of Periodontal Pathogens on Hydroxyapatite Surfaces: Implications for Periodontium Damage. *J. Biomed. Mater. Res. A* **2016**, *104*, 2873−2880.
(33) Darrene, L.-N.; Cecile, B. Experimental Models of Oral Biofilms Developed on Inert Substrates: A Review of the Literature. *BioMed Res. Int.* **2016**, *2016*, 1−8.
(34) de Sousa, D. L.; Lima, R. A.; Zanin, I. C.; Klein, M. I.; Janal, M. N.; Duarte, S. Effect of Twice-daily Blue Light Treatment on Matrix-rich Biofilm Development. *PLoS One* **2015**, *10*, No. e0131941.
(35) Wasserman, H. H.; Larsen, D. L. Formation of 1,4-endoperoxides from the dye-sensitized photo-oxygenation of alkylnaphthalenes. *J. Chem. Soc., Chem. Commun.* **1972**, 253−254.
(36) Aubry, J.-M.; Pierlot, C.; Rigaudy, J.; Schmidt, R. Reversible Binding of Oxygen to Aromatic Compounds. *Acc. Chem. Res.* **2003**, *36*, 668−675.
(37) Di Mascio, P.; Miyamoto, S.; Medeiros, M. G. H.; Martinez, G. R.; Cadet, J. Chemistry Functional Groups in Organic Chemistry. In *The Chemistry of Peroxides*; Greer, A., Liebman, J. F., Eds.; Wiley, 2014; Vol. *3*, pp 769−804.
(38) Turro, N. J.; Ramamurthy, V.; Scaiano, J. C. *Modern Molecular Photochemistry of Organic Molecules*; University Science Books: Sausalito, CA, 2010; pp 1001−1040.
(39) Lindig, B. A.; Rodgers, M. A. J.; Schaap, A. P. Determination of the lifetime of singlet oxygen in water-d_2 using 9,10-anthracenedipropionic acid, a water-soluble probe. *J. Am. Chem. Soc.* **1980**, *102*, 5590−5593.
(40) Lindig, B. A.; Rodgers, M. A. J. Rate parameters for the quenching of singlet oxygen by water-soluble and lipid-soluble substrates in aqueous and micellar systems. *Photochem. Photobiol.* **1981**, *33*, 627−634.
(41) Ruiz-González, R.; Cortajarena, A. L.; Mejias, S. H.; Agut, M.; Nonell, S.; Flors, C. Singlet Oxygen Generation by the Genetically Encoded Tag miniSOG. *J. Am. Chem. Soc.* **2013**, *135*, 9564−9567.
(42) Ogilby, P. R.; Foote, C. S. Chemistry of singlet oxygen. 42. Effect of solvent, solvent isotopic substitution, and temperature on the lifetime of singlet molecular oxygen (1.DELTA.g). *J. Am. Chem. Soc.* **1983**, *105*, 3423−3430.
(43) Jensen, R. L.; Arnbjerg, J.; Ogilby, P. R. Temperature Effects on the Solvent-Dependent Deactivation of Singlet Oxygen. *J. Am. Chem. Soc.* **2010**, *132*, 8098−8105.
(44) Day, R. A.; Estabrook, D. A.; Logan, J. K.; Sletten, E. M. Fluorous photosensitizers enhance photodynamic therapy with perfluorocarbon nanoemulsions. *Chem. Commun.* **2017**, *53*, 13043−13046.
(45) Kimel, S.; Tromberg, B. J.; Roberts, W. G.; Berns, M. W. Singlet oxygen generation of porphyrins, chlorins, and phthalocyanines. *Photochem. Photobiol.* **1989**, *50*, 175−183.
(46) Kruft, B. I.; Greer, A. Photosensitization Reactions In Vitro and In Vivo. *Photochem. Photobiol.* **2011**, *87*, 1204−1213.
(47) Roberts, W. G.; Shiau, F.-Y.; Nelson, J. S.; Smith, K. M.; Berns, M. W. In Vitro Characterization of Monoaspartyl Chlorin e6 and Diaspartyl Chlorin e6 for Photodynamic Therapy. *J. Natl. Cancer Inst.* **1988**, *80*, 330−336.
(48) Spikes, J. D.; Bommer, J. C. Photosensitizing Properties of Mono-L-Aspartyl Chlorin e6 (NPe6): A Candidate Sensitizer for the Photodynamic Therapy of Tumors. *J. Photochem. Photobiol., B* **1993**, *17*, 135−143.
(49) Hamblin, M. R.; Miller, J. L.; Rizvi, I.; Ortel, B.; Maytin, E. V.; Hassan, T. Pegylation of a Chlorin e_6 Polymer Conjugate Increases Tumor Targeting of Photosensitizer. *Cancer Res.* **2001**, *61*, 7155−7162.
(50) Nyokong, T. Effects of Substituents on the Photochemical and Photophysical Properties of Main Group Metal Phthalocyanines. *Coord. Chem. Rev.* **2007**, *251*, 1707−1722.
(51) Zhao, B.; Yin, J.-J.; Bilski, P. J.; Chignell, C. F.; Roberts, J. E.; He, Y.-Y. Enhanced Photodynamic Efficacy Towards Melanoma Cells by Encapsulation of Pc4 in Silica Nanoparticles. *Toxicol. Appl. Pharmacol.* **2009**, *241*, 163−172.
(52) Dror, S. B.; Bronshtein, I.; Garini, Y.; O'Neal, W. G.; Jacobi, P. A.; Ehrenberg, B. The Localization and Photosensitization of Modified Chlorin Photosensitizers in Artificial Membranes. *Photochem. Photobiol. Sci.* **2009**, *8*, 354−361.
(53) Jux, N.; Röder, B. Targeting Strategies for Tetrapyrrole-Based Photodynamic Therapy. In *Handbook of Porphyrin Science*; Kadish, K. M., Smith, K. M., Guilard, R., Eds.; World Scientific Publishing Co. Ltd.: Singapore, 2010; Vol. *4*, pp 325−401.
(54) Senge, M. O.; Brandt, J. C. Temoporfin (Foscan, 5,10,15,20-Tetra(m-hydroxyphenyl)chlorin)-A Second-generation Photosensitizer. *Photochem. Photobiol.* **2011**, *87*, 1240−1296.
(55) Kimani, S.; Ghosh, G.; Ghogare, A.; Rudshteyn, B.; Bartusik, D.; Hasan, T.; Greer, A. Synthesis and Characterization of Mono-, Di-, and Tri-Poly(ethylene glycol) Chlorin e6 Conjugates for the Photokilling of Human Ovarian Cancer Cells. *J. Org. Chem.* **2012**, *77*, 10638−10647.
(56) Anula, H. M.; Berlin, J. C.; Wu, H.; Li, Y.-S.; Peng, X.; Kenney, M. E.; Rodgers, M. A. J. Synthesis and Photophysical Properties of Silicon Phthalocyanines with Axial Siloxy Ligands Bearing Alkylamine Termini. *J. Phys. Chem. A* **2006**, *110*, 5215−5223.
(57) Girotti, A. W.; Korytowski, W. Reactions of Singlet Oxygen with Membrane Lipids: Lipid Hydroperoxide Generation, Translocation, Reductive Turnover, and Signaling Activity. *Singlet Oxygen: Applications in Biosciences and Nanosciences*; Comprehensive Series in Photochemical & Photobiological Sciences; RSC publishing, 2016; Vol. *1*, pp 409−430.
(58) Greer, A. Christopher Foote's Discovery of the Role of Singlet Oxygen [$^1O_2(^1\Delta_g)$] in Photosensitized Oxidation Reactions. *Acc. Chem. Res.* **2006**, *39*, 797−804.
(59) Renikuntla, B. R.; Rose, H. C.; Eldo, J.; Waggoner, A. S.; Armitage, B. A. Improved Photostability and Fluorescence Properties Through Polyfluorination of a Cyanine Dye. *Org. Lett.* **2004**, *6*, 909−912.
(60) Georgakoudi, I.; Foster, T. H. Singlet Oxygen-Versus Nonsinglet Oxygen-Mediated Mechanisms of Sensitizer Photobleaching and Their Effects on Photodynamic Dosimetry. *Photochem. Photobiol.* **1998**, *67*, 612−625.

DOI: 10.1021/acsami.8b09439
ACS Appl. Mater. Interfaces 2018, 10, 25819−25829

(61) Rotomskis, R.; Streckyte, G.; Bagdonas, S. Phototransformations of sensitizers 1. Significance of the nature of the sensitizer in the photobleaching process and photoproduct formation in aqueous solution. *J. Photochem. Photobiol., B* **1997**, *39*, 167−171.
(62) Fernandez, J. M.; Bilgin, M. D.; Grossweiner, L. I. Singlet Oxygen Generation by Photodynamic Agents. *J. Photochem. Photobiol., B* **1997**, *37*, 131−140.
(63) Li, M.; Mai, B.; Wang, A.; Gao, Y.; Wang, X.; Liu, X.; Song, S.; Liu, Q.; Wei, S.; Wang, P. Photodynamic Antimicrobial Chemotherapy with Cationic Phthalocyanines against *Escherichia coli* Planktonic and Biofilm Cultures. *RSC Adv.* **2017**, *7*, 40734−40744.
(64) Tunér, J.; Ribeiro, M. S.; Simões, A. Dosimetry. In *Lasers in Dentistry: Guide for Clinical Practice*, 1st ed.; de Freitas, P. M., Simões, A., Eds.; John Wiley & Sons, Inc., 2015; Chapter 8, pp 48−55.
(65) Schaap, A. P.; Thayer, A. L.; Blossey, E. C.; Neckers, D. C. Polymer-Based Sensitizers for Photooxidations. II. *J. Am. Chem. Soc.* **1975**, *97*, 3741−3745.
(66) Protti, S.; Albini, A.; Viswanathan, R.; Greer, A. Targeting Photochemical Scalpels or Lancets in the Photodynamic Therapy Field-The Photochemist's Role. *Photochem. Photobiol.* **2017**, *93*, 1139−1153.

DOI: 10.1021/acsami.8b09439
ACS Appl. Mater. Interfaces 2018, 10, 25819−25829